Nonlinear Dyn (2007) 50:431–445
DOI 10.1007/s11071-006-9190-1

ORIGINAL ARTICLE

Poincaré maps modeling and local orbital stability analysis of discontinuous piecewise affine periodically driven systems

Abdelali El Aroudi · Mohamed Debbat · Luis Martinez-Salamero

Received: 26 April 2006 / Accepted: 12 September 2006 / Published online: 26 January 2007

Abstract This paper presents a methodology to study the local stability of periodic orbits (orbital stability) in switched discontinuous piecewise affine (DPWA) periodically driven multiple-input multiple-output (MIMO) systems. The switched system of interest has a bilinear state space representation where the controller inputs are binary signals taking values in the set $\{0,1\}$. These systems are characterized by a set of affine differential equations together with switching rules to commute between them. These switching rules are described by switching functions that are periodic in time and linear in state. The methodology is based on obtaining a discrete time model (Poincaré map), its steady state operation points, and its Jacobian matrix. This provides a powerful tool for studying their stability and to predict some kind of instability phenomena that the system can undergo like subharmonic oscillations. The proposed approach is applied to a power electronic circuit which toggles among six different system equations with five switching boundaries within a switching cycle.

This work was supported by the Spanish *Ministerio de Educación y Ciencia under Grant* TEC-2004-05608-C02-02.

A. El Aroudi (✉) · M. Debbat · L. Martinez-Salamero
Departament d'Enginyeria Electrònica, Elèctrica i Automàtica (DEEEA), Grupo de Automática y Electrónica Industrial (GAEI), Universitat Rovira i Virgili, Tarragona, Spain
e-mail: abdelali.elaroudi@urv.net

Keywords MIMO systems · Piecewise affine systems · Discontinuous systems · Switched systems · Periodically driven systems · Stability analysis · Discrete time modeling · Poincaré map

1 Introduction

Many problems in applied science and control engineering result in the consideration of switched systems. Variable structure system control, sliding mode control, relay control, gain scheduling, bang–bang control, and fuzzy logic control are examples of control techniques that lead to a switched system. The common characteristic for all of them is the switching between different configurations. A special case of these systems is the class of piecewise linear (PWL) systems. The last one has been a subject of research in the systems and control community for a long time, see for example refs. [1–6] and references therein. PWL switched systems constitute a special class of hybrid systems [3, 7] and arise often in practical control systems when some nonlinear components such as switching, dead-zone, saturation, relays, and hysteresis are encountered. Most of the PWL systems studied in the literature are characterized by switching among linear configurations when certain fixed boundaries in the state space are reached. The stationary behavior of such systems could be an equilibrium point at the origin or a more complex orbit in its vicinity. The fundamental frequency component of this orbit depends on the parameters of the system

and are not fixed by the controller. Sometimes, the study of such systems is carried out using the continuous time approach from the equations describing the flow of the system by assuming continuity in the vector field [8] or by assuming the existence of sliding mode in the case of discontinuous vector field (Filippov Systems) [9]. However, in many cases, the vector field is discontinuous but sliding mode may not always exist. This results in a handicap for making a rigorous mathematical analysis of wide class of switched systems using continuous time approach. Very often, each configuration is not linear but affine. Moreover, in many systems, the boundaries are periodically moving in the state space [10] and the vector field may be discontinuous at one or more of the switching boundaries. The overall system is called Discontinuous Piecewise Affine (DPWA) periodically driven system. When the number of the switching boundaries is more than 1, we are dealing with multiple-input multiple-output (MIMO) DPWA systems that are more general than simple PWL systems. DPWA systems are frequently encountered in many fields of science and engineering, where relationships among relevant variables are affine in one region but can be of different nature in some other regions of the state space. The discontinuity of the vector field at the switching boundary implies that $\dot{\mathbf{x}}_k^-$ the derivative of the state variables just before switching are different from the derivatives $\dot{\mathbf{x}}_k^+$ just after switching. Examples of DPWA systems are ON–OFF systems like power electronic converters [11–18], chemical reactors [19], and variable structure control systems [20–22].

The mathematical analysis of the system by using averaging techniques is possible but this does not give accurate conclusions about stability and performances [23]. An alternative approach for studying a wide class of these systems accurately is by using the discrete time model which can be obtained from the differential equations describing the flow in the continuous time domain. Although widely used, very few results are available to analyze the stability of general MIMO DPWA systems with Poincaré maps and very often the study of these systems is done case by case. As a matter of fact, properties of such systems like stability of the stationary operating regime and dynamic performance are inferred from extensive and very time-consuming computer simulations. In refs. [10–13], Poincaré map modeling was applied to DC–DC elementary power converters with two or three switching configurations. However, many power electronics circuits and other systems could be characterized by more than three cyclic configurations [18, 24]. The aim of this work is to give a general methodology to obtain the Poincaré map and its Jacobian matrix of a wider class of systems than those considered in refs. [1–9]. The fixed point and the Jacobian matrix of this model are given in closed form in terms of the stationary switching instants. We will show that instabilities in the form of generic bifurcations like flip bifurcation (FB) and Neimark–Sacker bifurcation (NSB) can be detected accurately. The proposed approach is applied to analyze the stability of a practical power electronic circuit with six affine configurations and whose corresponding vector field is discontinuous through the switching boundary. The remainder of the paper is organized as follows. Section 2 will deal with the problem description. In Section 3, we present a systematic procedure to obtain the Poincaré map approach for MIMO DPWA systems. The fixed points and the Jacobian matrix are given in Section 4. An example is presented in Section 5. This example shows that the nominal periodic orbit of MIMO DPWA systems that are nonsmooth are present at first bifurcation phenomena which are typical in smooth systems. However, after the occurrence of the first bifurcation, many other nonsmooth bifurcations like border collisions take place. This paper will not discuss in detail the mathematical tools for nonsmooth analysis. This will be a benefit to nonspecialist readers and allowing at the same time to represent a wide class of systems in a more accessible manner. Finally, some conclusions are drawn in the last section.

2 Discontinuous piecewise affine periodically driven systems

Most dynamical systems found in control engineering, power electronics circuits, and neurons can be considered as systems whose structure changes when some conditions on the state variables and/or time are fulfilled. In this work, we are interested in a class of DPWA systems that are characterized by a finite number of affine dynamical models together with a set of switching conditions to toggle among these models. This model description produces a partitioning of the state space into different cells. Within each cell, the dynamics are described generally by a different affine equation. At boundaries between two adjacent

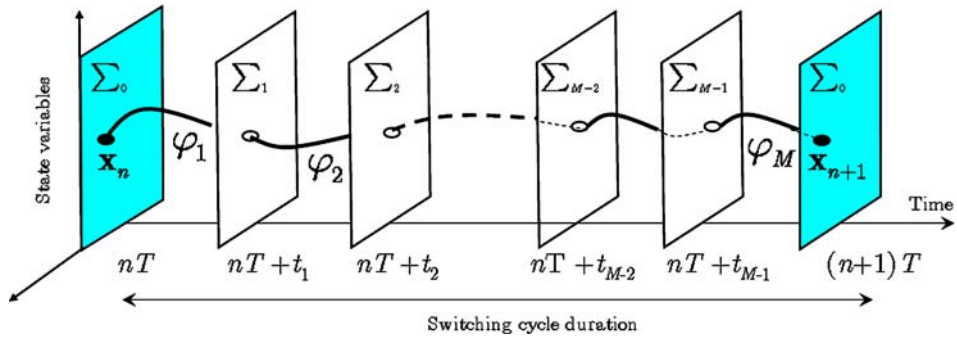

Fig. 1 Partitioning of the state space into different cells. Each cell has a distinctive flow description

cells, the system switches from one affine configuration to another and due to discontinuity of the vector field smoothness is lost when a trajectory crosses these boundaries which are called, therefore, nonsmoothness sets or switching manifolds. Consider a MIMO DPWA system with m inputs and M–1 switching conditions and generally M different configurations within one switching cycle (Fig. 1). Let us suppose that the switching from one configuration C_k to another one C_{k+1} forms a well determined and fixed sequence:

$$\mathrm{C_1} \rightarrow \mathrm{C_2} \cdots \rightarrow \mathrm{C_M} \rightarrow \mathrm{C_1} \rightarrow \mathrm{C_2} \cdots \mathrm{C_M} \rightarrow \cdots \quad (1)$$

During each configuration, the system is governed by an affine time-invariant equation of the following form:

$$\dot{\mathbf{x}} = \mathbf{A}_k \mathbf{x} + \mathbf{B}_k \quad (2)$$

where $\mathbf{x} \in \mathbf{R}^N$ is the vector of state variables, and $\mathbf{A}_k \in \mathbf{R}^{N\times N}$ and $\mathbf{B}_k \in \mathbf{R}^{N\times 1}$ are the system matrices and vectors during each phase and whose components are the system parameters. All eigenvalues of each matrix $\mathbf{A}_k$ are assumed to be located in the left-half side of the complex plane or have a single eigenvalue at the origin. This assumption is related to the fact that each affine configuration is a model of a dissipative physical system.

Assumption. Throughout this paper, we assume that the steady state regime is characterized by switching functions so that in each cycle, $M-1$ actual switching moments are present. If this is not the case, it means that there are some skipped switching in the system for one or more periods. This may lead to situations for which the system is not working properly.

A compact form expression may be written as follows:

$$\dot{\mathbf{x}} = \mathbf{A}\mathbf{x} + \mathbf{B}\mathbf{x}\mathbf{u} + \mathbf{C}\mathbf{u} + \mathbf{D} \quad (3)$$

where $\mathbf{A} \in \mathbf{R}^{N\times N}$, $\mathbf{B} \in \mathbf{R}^{N\times m}$, $\mathbf{C} \in \mathbf{R}^{N\times m}$, and $\mathbf{D} \in \mathbf{R}^N$. $\mathbf{u} \in \mathbf{R}^m$ is the vector of binary input signals. m is the number of inputs in the system. Equation (3) is the bilinear state space representation in which the control inputs are binary signals taking values in the set $\{0,1\}$. This is the general form of systems of interest in this paper. Note that by giving to the components of $\mathbf{u}$ values in the set $\{0,1\}$, we will get an equation of the form of Equation (2).

These kinds of systems are more general than those studied in refs. [3, 10–13] and other related works in hybrid systems literature.

In open-loop systems, the entries in the vector input $\mathbf{u}$ are external periodic piecewise constant signals u_k, $k = 1, \ldots, m$. In this case, the average value of output variables during a switching cycle undergoes variations under parameter changes. The control objective in this kind of systems is to drive the system to a periodic orbit with a fixed frequency in steady state and with a desired average value of the state variables. This is accomplished by generating the driving signals u_k from the own state variables by comparing their corresponding errors with suitable repetitive signals like in Pulse Width Modulation (PWM) control method. Across the switching manifolds, the system can be characterized by different order of discontinuities in the vector field. We have the following cases:

- systems with discontinuous state variables $\mathbf{x}$, i.e., for some switching instant t_k and corresponding

switching manifold Σ_k, one can have:

$$\forall t_k / \mathbf{x}(t_k) \in \Sigma_k, \quad \mathbf{x}(t_k^-) \neq \mathbf{x}(t_k^+).$$

These systems are usually studied by the so-called discontinuity map [24].

- systems with continuous state variables but discontinuous vector fields i.e., for some switching instant t_k and corresponding switching manifold Σ_k, one can have:

$$f_k(\mathbf{x}(t_k)) \neq f_{k+1}(\mathbf{x}(t_k)).$$

These systems are called Filippov systems and are traditionally studied by using sliding mode if the switching boundaries are fixed [21] and averaging techniques [16] if the switching boundaries are periodically time varying like those considered in this paper. The generalized Jacobian matrix, taking into account discontinuity at the switching boundary, could also be used [9]. Here, the first class of systems which are discontinuous in the state $\mathbf{x}$, are not considered. These systems are called Impulsive Differential Equations (IDE) and are characterized by a Dirac impulse function $\delta(\mathbf{x})$ in their vector fields. The switching moments t_k may be fixed a priori or given as a solution of a switching equation like $\sigma_k(\mathbf{x}, t_k) = 0$. If all t_k are given in a fixed pattern, the system is called open loop. If for some k, t_k is given as the result of a crossing between a control signal s_k and an external periodic signal h_k, the system is closed loop. This is the most important case because many practical systems in industrial applications are designed to work in closed loop. Controller design and stability analysis requires an appropriate dynamics model. For DPWA systems, the switched mode is highly nonlinear making the stability analysis and control design a very difficult task. Because in these systems, the dynamic model involves periodically varying quantities even at steady state operation, one way to get a constant steady state is by using a discrete time model in the form of a Poincaré map. This can be obtained by sampling the state variables at the switching period. The averaging techniques can also be used to get a constant steady state but they are not accurate. Discrete time modeling in the form of Poincaré mapping of these systems is usually restricted to systems with low order and number of configurations. In the following sections, we will give a general systematic procedure to get the Poincaré map of these systems.

3 Poincaré map of the open-loop system

In open-loop systems the time moments t_k are given a priori and the switching from one configuration to another is given in a fixed pattern. As Equation (2) is affine and time invariant, a closed-form solution is available and it can be written as:

$$\mathbf{x}(t) = \varphi_k(t, \mathbf{x}_0) \tag{4}$$

where $\mathbf{x}_0$ is an arbitrary initial condition. Assume that, during one switching cycle, the system changes its structure from f_k to f_{k+1} when the trajectory φ_k starting from initial condition $\mathbf{x}_{k-1}$ on a surface Σ_{k-1} reaches Σ_k at time instant t_k, measured by starting from the beginning of the kth cycle (Fig. 1). $\Sigma_k; k = 1, 2, \ldots, M$, are switching manifolds that are given by fixed switching moments. During one switching cycle, local maps $\mathbf{P}_k$ in the following form can be defined:

$$\begin{aligned}
&\mathbf{P}_1 : \Sigma_0 \to \Sigma_1 \\
&\quad \mathbf{x}_n \to \mathbf{x}(t_1) := \varphi_1(t_1, \mathbf{x}_n) \\
&\mathbf{P}_2 : \Sigma_1 \to \Sigma_2 \\
&\quad \mathbf{x}(t_1) \to \mathbf{x}(t_2) := \varphi_2(t_2 - t_1, \mathbf{x}(t_1)) \\
&\mathbf{P}_3 : \Sigma_2 \to \Sigma_3 \\
&\quad \mathbf{x}(t_2) \to \mathbf{x}(t_3) := \varphi_3(t_3 - t_2, \mathbf{x}(t_2)) \\
&\vdots \\
&\mathbf{P}_M : \Sigma_{M-1} \to \Sigma_0 \\
&\quad \mathbf{x}(t_{M-1}) \to \mathbf{x}_{n+1} := \varphi_M(T - t_{M-1}, \mathbf{x}(t_{M-1}))
\end{aligned} \tag{5}$$

where t_k $(k = 1, \ldots, M-1)$ are the switching instants measured from the beginning of the switching cycle and T is its period. A Poincaré map from Σ_0 to Σ_0, can be defined as the composition of the M different local mapping $\mathbf{P}_k$, i.e:

$$\mathbf{P} = \mathbf{P}_M \circ \mathbf{P}_{M-1} \circ \cdots \mathbf{P}_1. \tag{6}$$

This map can be expressed as:

$$\mathbf{P} : \Sigma_0 \to \Sigma_0$$

$$\mathbf{x}_{\mathrm{n}} \to \mathbf{x}_{n+1} := \mathbf{P}(\boldsymbol{\tau}, \mathbf{x}_n) = \varphi_M(T - t_{M-1}, \varphi_{M-1} \times (t_{M-1} - t_{M-2}, \varphi_{M-2}(\ldots))) \quad (7)$$

where $\boldsymbol{\tau} = (t_1, t_2\ t_{M-1})^t$ is the vector of the switching instants. As was mentioned earlier, we are considering here that the switching is due to the existence of some kind of T-periodic function. Thus, for the open-loop system, we can have only nominal periodic orbits with period T. Equilibrium points are possible only in the evident case when the system remains blocked in some configuration (without switching).

3.1 Existence conditions of periodic orbits

In a switched system with M different configurations, different types of periodic orbits may exist. But only some of them are desired from a practical point of view. Among all the possible periodic orbits for the system, the most interesting from an engineering point of view is the nominal one which is characterized by switching among M configurations during one switching cycle.

Definition. A periodic orbit that is characterized by M and only M different configurations during one switching cycle is called M-modal periodic orbit. An M-modal periodic orbit $\mathbf{x}^*(t)$ will exist if there exists a vector $(t_1, t_2, \ldots, t_{M-1})$, such that the following conditions hold:

1. $\mathbf{x}^*(kT) = \mathbf{x}^*((k+1)T) \forall k = 1, \ldots, M$
2. $\dot{\mathbf{x}}^*(t) = \mathbf{A}_k \mathbf{x}^*(t) + \mathbf{B}_k$ for $t \in (t_{k-1}, t_k)$ $\forall k = 1, \ldots, M$

3.2 Poincaré map for periodic orbits: fixed points

The usefulness of the Poincaré map results from the fact that its fixed points $\mathbf{X}^*$ correspond to periodic orbits $\mathbf{x}^*$ of the continuous time-switched system and that the stability properties are the same for both of them. The piecewise affine character of this class of systems allows us also to obtain the fixed points of $\mathbf{P}$ in terms of time instants t_k. Generally, function φ_k can be written as:

$$\varphi(t, \mathbf{x}_{k-1}) = \phi_k(t)\mathbf{x}_{k-1} + \psi(t)\mathbf{B}_k \quad (8)$$

where matrices ϕ and ψ are given as follows:

$$\phi(t) = e^{\mathbf{A}t},\ \psi(t) = \int_0^t e^{\mathbf{A}\alpha} d\alpha \quad (9)$$

Note that the matrix ψ is well defined by Equation (9) even if $\mathbf{A}$ is singular. If $\mathbf{A}$ is invertible, the matrix function ψ can be written as:

$$\psi(t) = \mathbf{A}^{-1}(\phi(t) - \mathbf{1}) \quad (10)$$

where $\mathbf{1}$ is the identity matrix with appropriate dimension. In the case of a singular matrix $\mathbf{A}$, we have from Equation (9) and using time series expansion of the matrix exponential:

$$\psi(t) = \left(\mathbf{1}t + \frac{\mathbf{A}t^2}{2} + \frac{\mathbf{A}^2 t^3}{6} + \cdots + \frac{\mathbf{A}^k t^{k+1}}{(k+1)!} + \cdots\right). \quad (11)$$

Independently of whether $\mathbf{A}$ is invertible or not, the expression of map $\mathbf{P}$ can be written in the following form:

$$\begin{aligned} &\mathbf{P}\colon \Sigma_0 \to \Sigma_0 \\ &\quad \mathbf{x}_{\mathrm{n}} \to \mathbf{P}(\mathbf{d}, \mathbf{x}_n) = \phi_M(d_M)[\phi_{M-1}(d_{M-1}) \\ &\qquad \times (\cdots \phi_2(d_2)(\phi_1(d_1)\mathbf{x}_n + \psi_1(d_1)\mathbf{B}_1) \\ &\qquad + \psi_2(d_2)\mathbf{B}_2) \cdots + \cdots \psi_{M-1}(d_{M-1})\mathbf{B}_{M-1}] \\ &\qquad + \cdots + \psi_M(d_M)\mathbf{B}_M \end{aligned} \quad (12)$$

where

$$\begin{aligned} &d_1 = t_1 \\ &d_k = t_k - t_{k-1} \quad \text{for } 2 < k < M-1 \quad \text{and} \\ &d_M = T - t_{M-1}. \end{aligned}$$

If we collect the time durations d_k in a column vector $\mathbf{d} = (d_1, d_2, \ldots, d_M)^t$ and perform some algebra, Equation (12) can be written as follows:

$$\mathbf{P}(\mathbf{d}, \mathbf{x}_n) = \Phi(\mathbf{d})\mathbf{x}_n + \Psi(\mathbf{d}) \quad (13)$$

where

$$\Phi(\mathbf{d}) = \prod_{k=M}^{1} \phi_k(d_k) \quad (14)$$

and

$$\Psi(\mathbf{d}) = \sum_{j=1}^{M-1} \prod_{k=M}^{j+1} \phi_k(d_k)\psi_j(d_j)\mathbf{B}_j + \psi_M(d_M)\mathbf{B}_M. \quad (15)$$

A fixed point of $\mathbf{P}$ is a point $\mathbf{X}^*$ in the state space for which we have $\mathbf{X}^* = \mathbf{P}(\mathbf{X}^*, \mathbf{d}^*)$. Using the expression of $\mathbf{P}$, $\mathbf{X}^*$ can be expressed in terms of the vector of steady state time durations $\mathbf{d}^*$, corresponding to fixed points $\mathbf{X}^*$ and matrices Φ and Ψ evaluated at $\mathbf{d}^*$

$$\mathbf{X}^*(\mathbf{d}^*) = (\mathbf{1} - \Phi(\mathbf{d}^*))^{-1} \cdot \Psi(\mathbf{d}^*). \quad (16)$$

It should be noted here that the fixed point and hence its associated M-modal periodic orbit exists and it is unique whenever the inverse in Equation (16) exists, i.e, if the matrix $\mathbf{1} - \Phi(\mathbf{d}^*)$ is not singular. Note also that in this case only one solution for the switching equations may exist and this gives rise to only one fixed point $\mathbf{X}^*$. This is because the open-loop system is linear.

The stability of periodic orbits $\mathbf{x}^*$ is the same as for fixed points $\mathbf{X}^*$ of the map $\mathbf{P}$. This can be investigated using the Jacobian matrix $\mathbf{DP}$ of the map $\mathbf{P}$. This matrix relates how an infinitely small perturbation near $\mathbf{X}^*$ at the beginning of a switching cycle causes a final perturbation at the end of the same cycle. The fixed point $\mathbf{X}^*$and then the periodic solution will be stable if the eigenvalues (the characteristic multipliers) of the Jacobian matrix lie inside the unit circle.

The piecewise affinity and time invariance of the system allow the obtaining of $\mathbf{DP}$ in closed form in terms of t_k. In the open loop case, all these time instants are given in a fixed pattern, and $\mathbf{DP}$ can be expressed as the product of the Jacobian matrix of each local map. By differentiating Equation (13) with respect to the discrete state variables $\mathbf{x}_n$, we obtain the Jacobian matrix $\mathbf{DP}$ as:

$$\mathbf{DP} = \Phi(\mathbf{d}) = \prod_{k=M}^{1} \phi_k(d_k). \quad (17)$$

It can be observed in this case that the asymptotic stability of the switched system will be assured if each affine configuration is asymptotically stable. That is to say, if all matrices $\mathbf{A}_k$ have all eigenvalues in the left-half side of the complex plane, all the eigenvalues of $\Phi(\mathbf{d}^*)$ will be inside the unit circle.

4 Stability of periodic orbits in the closed-loop system

In closed-loop systems, some of the time instants t_k depend on the state variables linearly or by some nonlinear form depending on the controller. Let us suppose that, in the closed-loop system, the switching functions σ_k defining the switching manifolds Σ_k can be written as the difference between a state dependent function s_k ($\mathbf{x}$) and a time-dependent T-periodic function h_k, i.e:

$$\Sigma_k = \{\mathbf{x} \in \mathbf{R}^n / \sigma_k(t, \mathbf{x}) := s_k(\mathbf{x}) - h_k(t) = 0\} \quad (18)$$

Generally, functions s_k defining the switching manifolds Σ_k could take any form. However, for the sake of clarity, we will suppose here that they are linear functions of the errors of the state variables and, thus, they can be written as s_k ($\mathbf{x}$) = $\mathbf{K}_k$ ($\mathbf{X}_{\mathrm{ref},k}$-$\mathbf{x}$), where $\mathbf{K}_k$ are suitable feedback coefficients during the switching kth subinterval that are selected with the purpose to control some output variables and $\mathbf{X}_{\mathrm{ref},k}$ is the vector of the reference trajectory in the kth subinterval. The functions h_k are, without loss of generality, piecewise linear T-periodic signals of time that are used together with the error signals to get a desired stationary average value of the output variables and the desired switching period T for the state variables. Note that as the switching condition is given by a nonlinear equation, there can exist more than one set of switching instants and therefore more than one M-modal periodic orbit. Next, we focus on the presence of a M-modal periodic orbit for the system in closed loop. Given such a periodic orbit, the switching instants in each period, determined by the feedback, are fixed in steady state. Once these fixed instants are known, the associated periodic orbit can be computed. Hence, the stationary switching instants are determined by the associated periodic orbit through the applied switching functions, and conversely, the stationary switching instants determine the periodic orbit. Therefore, in order to compute the periodic orbit and the associated stationary switching instants, we have to find a solution for a set of transcendental equations consisting of the equations imposed by the stationary orbit that depend on the stationary switching instants, and the equation by which the stationary switching instants can be obtained from the feedback based on the periodic orbit. As these equations are nonlinear, it turns out that depending on the value of the parameters there can be more than one periodic orbit, some of which would not

be necessarily stable. Moreover, the stability issue is now a local matter, whereas in the open-loop situation stability was global. Usually, it is not possible to obtain a closed-form expression for these instants. Obtaining the fixed point $\mathbf{X}^*$ requires solving a set of transcendental equations $\sigma(\mathbf{X}^*, \boldsymbol{\tau}^*) = 0$ where $\sigma(\mathbf{X}^*,\boldsymbol{\tau}^*)$ is a vector of switching functions given by:

$$\boldsymbol{\sigma}(\boldsymbol{\tau}^*, \mathbf{X}^*) = \begin{pmatrix} \mathbf{K}_1(\mathbf{X}_{\text{ref},1} - \mathbf{P}_1(\mathbf{X}^*, t_1^*)) - h_1(t_1^*) \\ \mathbf{K}_2(\mathbf{X}_{\text{ref},2} - \mathbf{P}_2 \circ \mathbf{P}_1(\mathbf{X}^*, t_1^*, t_2^*)) - h_2(t_2^*) \\ \vdots \\ \mathbf{K}_{M-1}(\mathbf{X}_{\text{ref},M-1} - \mathbf{P}_{M-1} \circ \mathbf{P}_{M-2} \circ \cdots \circ \\ \quad \mathbf{P}_1(\mathbf{X}^*, t_1^*, t_2^*, \ldots t_{M-1}^*)) - h_{M-1}(t_{M-1}^*) \end{pmatrix} \tag{19}$$

where $\mathbf{X}^*$ is given by Equation (16). Therefore, a root finding algorithm should be applied to Equation (19) to obtain $\boldsymbol{\tau}^* = (t_1^*, t_2^*, \ldots t_{M-1}^*)$. For instance, the least squares method can be used after substituting the local mappings $\mathbf{P}_k$ by their expressions. The problem can be treated as an optimization process where the objective function to be minimized is $\sigma(\boldsymbol{\tau}^*)$ and the parameters to be optimized are switching time instants t_k, $(k = 1, \ldots, M-1)$, with the constraints $0 < t_k < T$. The process can be started from $M-1$ equidistant switching instants in the interval $(0, T)$, i.e: $\boldsymbol{\tau}_0 = (\frac{T}{M}, \frac{2T}{M}, \cdots \frac{(M-1)T}{M})^t$. The optimal solution $\boldsymbol{\tau}^*$ for the vector of switching instants is then substituted in Equation (16) to obtain the fixed point $\mathbf{X}^*$. Once this fixed point is located, its stability analysis may be carried out by studying the local behavior of the map $\mathbf{P}$ in its vicinity. In closed-loop systems, switching time instants t_k depend on the discrete state variables $\mathbf{x}_n$ in a nonlinear form. The dependence of these instants on the discrete state variables changes the nature of the map $\mathbf{P}$ from a linear map to a nonlinear one. The expression of the Jacobian matrix $\mathbf{DP}$ is also modified by the presence of terms containing the derivative of the vector of switching instants $\boldsymbol{\tau}$ with respect to the vector of the discrete state variables $\mathbf{x}_n$. In this case, the expression of the Jacobian matrix becomes:

$$\mathbf{DP} = \Phi(\mathbf{d}) + \frac{\partial \mathbf{P}}{\partial \boldsymbol{\tau}} \frac{\partial \boldsymbol{\tau}}{\partial \mathbf{x}_n}. \tag{20}$$

Note that if the open loop system is stable, it is the second term in the expression of the Jacobian matrix that could introduce instability into the system. This fact can be explored in designing a stable closed-loop system by adjusting the parameters appearing in this term in order to make it as small as possible. However, some performances could be lost as we are then making the system to operate like in open loop. It is worth mentioning here that in the case of a digital controller, closed-form expression of $\boldsymbol{\tau}$ in terms of $\mathbf{x}_n$ is available and then explicit differentiation of $\boldsymbol{\tau}$ with respect to $\mathbf{x}_n$ is possible. In this case, we have:

$$t_k = \mathbf{K}_k(\mathbf{X}_{\text{ref},k} - \mathbf{x}_n). \tag{21}$$

From Equation (21), we have

$$\frac{\partial \boldsymbol{\sigma}(\boldsymbol{\tau}^*, \mathbf{X}^*)}{\partial \mathbf{x}_n} = -\begin{pmatrix} \mathbf{K}_1 \\ \mathbf{K}_2 \\ \vdots \\ \mathbf{K}_{M-1} \end{pmatrix} \tag{22}$$

In the case of analogue control methods, explicit differentiation of $\boldsymbol{\tau}$ with respect to $\mathbf{x}_n$ is not possible. However, the implicit function theorem allows us to write:

$$\frac{\partial \boldsymbol{\tau}}{\partial \mathbf{x}_n} = -\left(\frac{\partial \boldsymbol{\sigma}}{\partial \boldsymbol{\tau}}\right)^{-1} \left(\frac{\partial \boldsymbol{\sigma}}{\partial \mathbf{x}_n}\right). \tag{23}$$

Then, the expression of $\mathbf{DP}$ becomes:

$$\mathbf{DP} = \boldsymbol{\Phi}(\mathbf{d}) - \frac{\partial \mathbf{P}}{\partial \boldsymbol{\tau}} \left(\frac{\partial \boldsymbol{\sigma}}{\partial \boldsymbol{\tau}}\right)^{-1} \left(\frac{\partial \boldsymbol{\sigma}}{\partial \mathbf{x}_n}\right) \tag{24}$$

where σ is the column vector $[\sigma_k]$, $k = 1, \ldots, M-1$, given by:

$$\boldsymbol{\sigma}(\boldsymbol{\tau}, \mathbf{x}_n) = \begin{pmatrix} \mathbf{K}_1(\mathbf{X}_{\text{ref},1} - \mathbf{P}_1(\mathbf{x}_n, t_1)) - h_1(t_1) \\ \mathbf{K}_2(\mathbf{X}_{\text{ref},2} - \mathbf{P}_2 \circ \mathbf{P}_1(\mathbf{x}_n, t_1, t_2)) - h_2(t_2) \\ \vdots \\ \mathbf{K}_{M-1}(\mathbf{X}_{\text{ref},M-1} - \mathbf{P}_{M-1} \circ \mathbf{P}_{M-2} \circ \cdots \circ \\ \quad \mathbf{P}_1(\mathbf{x}_n, t_1, t_2, \ldots t_{M-1})) - h_{M-1}(t_{M-1}) \end{pmatrix} \tag{25}$$

By substituting the local mappings $\mathbf{P}_k$ by their corresponding expressions and differentiating the vector

of switching functions σ with respect to $\mathbf{x}_n$ we obtain:

$$\frac{\partial \boldsymbol{\sigma}(\boldsymbol{\tau}, \mathbf{x}_n)}{\partial \mathbf{x}_n} = \begin{pmatrix} \mathbf{K}_1\phi_1(t_1) \\ \mathbf{K}_2\phi_2(t_2 - t_1)\phi_1(t_1) \\ \vdots \\ \mathbf{K}_{M-1} \prod_{k=M-1}^{1} \phi_k(t_k - t_{k-1}) \end{pmatrix} \tag{26}$$

Likewise, by differentiating σ with respect to $\boldsymbol{\tau}$ we obtain:

$$\frac{\partial \boldsymbol{\sigma}(\boldsymbol{\tau}, \mathbf{x}_n)}{\partial \boldsymbol{\tau}} = \begin{pmatrix} -\mathbf{K}_1\dot{\mathbf{x}}_1^- - \dot{h}_1(t_1) & 0 & \cdots & 0 \\ -\mathbf{K}_2\phi_2\Delta\dot{\mathbf{x}}_1 & -\mathbf{K}_2\dot{\mathbf{x}}_2^- - \dot{h}_2(t_2) & \cdots & 0 \\ \vdots & \vdots & \ddots & \vdots \\ -\mathbf{K}_{M-1}\Delta\dot{\mathbf{y}}_1 & -\mathbf{K}_{M-1}\Delta\dot{\mathbf{y}}_2 & \cdots & -\mathbf{K}_{M-1}\dot{\mathbf{x}}_{M-1}^- - \dot{h}_{M-1}(t_{M-1}) \end{pmatrix} \tag{27}$$

where

$$\begin{aligned}
&\Delta\dot{\mathbf{x}}_k = \dot{\mathbf{x}}_k^- - \dot{\mathbf{x}}_k^+ \\
&\dot{\mathbf{x}}_1^- = \mathbf{A}_1\mathbf{P}_1(\mathbf{x}_n) + \mathbf{B}_1 \\
&\dot{\mathbf{x}}_1^+ = \mathbf{A}_2\mathbf{P}_2(\mathbf{x}_n) + \mathbf{B}_2 \\
&\dot{\mathbf{x}}_2^- = \mathbf{A}_2\mathbf{P}_2 \circ \mathbf{P}_1(\mathbf{x}_n) + \mathbf{B}_2 \\
&\dot{\mathbf{x}}_2^+ = \mathbf{A}_3\mathbf{P}_2 \circ \mathbf{P}_1(\mathbf{x}_n) + \mathbf{B}_3 \\
&\vdots \\
&\dot{\mathbf{x}}_{M-2}^- = \mathbf{A}_{M-2}\mathbf{P}_{M-2} \circ \mathbf{P}_{M-3} \circ \cdots \circ \mathbf{P}_1(\mathbf{x}_n) + \mathbf{B}_{M-2} \\
&\dot{\mathbf{x}}_{M-2}^+ = \mathbf{A}_{M-1}\mathbf{P}_{M-2} \circ \mathbf{P}_{M-3} \circ \cdots \circ \mathbf{P}_1(\mathbf{x}_n) + \mathbf{B}_{M-1} \\
&\dot{\mathbf{x}}_{M-1}^- = \mathbf{A}_{M-1}\mathbf{P}_{M-1} \circ \mathbf{P}_{M-2} \circ \cdots \circ \mathbf{P}_1(\mathbf{x}_n) + \mathbf{B}_{M-1} \\
&\Delta\dot{\mathbf{y}}_i = \prod_{k=M}^{i+1} \phi_k(d_k)\Delta\dot{\mathbf{x}}_i.
\end{aligned}$$

Note that as the vector field is discontinuous, the state variables derivative $\dot{\mathbf{x}}_k^-$ just before switching are different from the derivatives $\dot{\mathbf{x}}_k^+$ just after switching. This is reflected in the fact that $\Delta\dot{\mathbf{x}}_k \neq 0$ in this kind of systems. If such discontinuities do not exist, the matrix $\frac{\partial\boldsymbol{\sigma}}{\partial\boldsymbol{\tau}}$ will be diagonal. Finally, the partial derivative of the map function $\mathbf{P}$ with respect to $\boldsymbol{\tau}$ can be obtained from Equation (12) in the same way:

$$\frac{\partial \mathbf{P}}{\partial \boldsymbol{\tau}} = (\Delta\dot{\mathbf{y}}_1 \ \Delta\dot{\mathbf{y}}_2 \quad \cdots \quad \dot{\mathbf{x}}_{M-1}^-) \tag{28}$$

The continuity at the switching boundary will make all the components of Equation (28) null except the last one. This would simplify the computing of the Jacobian matrix for systems that do not present discontinuity at the switching boundary.

The stability analysis of the nominal periodic orbit of the closed loop system, represented by $\mathbf{X}^*$, can be carried out by using the eigenvalues of $\mathbf{DP}$ evaluated at the fixed point $\mathbf{X}^*$. This can be done by solving the characteristic equation for the fixed point $\mathbf{X}^*$ which is given by:

$$\det(\mathbf{DP} - \lambda\mathbf{1}) = 0 \tag{29}$$

A well-known condition for instability is that one of the eigenvalues has a modulus greater than 1. At a bifurcation point, the modulus of $\lambda = 1$ and we can write $\lambda = e^{j\theta}$. There are three standard ways for eigenvalues to leave the unit circle in the case of the smooth map P. For $\theta = \pi$, flip bifurcation (FB) takes place, while for $\theta = 0$, saddle-node bifurcation (SNB) can occur in which a pair of periodic orbits coalesce and disappear. For other values of θ, a Neimark–Sacker bifurcation (NSB) is possible.

5 Example: A four-level DC–DC buck power electronics converter under a MIMO PWM controller

The use of the Poincaré map to study the stability of periodic orbits in a power electronic circuit and to analyze their bifurcations was first done by Hamill et al. [25] where the deterministic model of the elementary (two level) DC–DC buck converter under a voltage-mode Pulse Width Modulation (PWM) control was addressed. It was shown in ref. [25] that the Poincaré map of the switched system, although very complex, does not involve discontinuities associated to the switching actions and results in a continuous map that can be

used to analyze accurately the stability of nominal periodic orbits. In the following subsections, we will apply the discrete time formulation presented previously to a four-level DC–DC buck converter. Note that the map **P** is smooth whenever the number of configurations does not change and the sequence is always the same.

5.1 System description

In order to validate the analytical expressions presented in the previous sections, let us consider the four-level DC–DC buck converter presented in Fig. 2. There are eight (2^3) different valid configurations depending on the state of the switches S_1, S_2, and S_3 and diodes D_1, D_2, and D_3. Different sequences and therefore different M-modal periodic orbits are possible depending on the duty cycles of the command signal and phase shift between them. These sequences define different operating modes of the converter. For a duty cycle between 33 and 50% and a phase shift of $2\pi/3$ between the command signals, the system toggles among six different affine and time-invariant configurations. These configurations are given in the Appendix. In order to perform the switch mode operation of the converter and with the purpose of regulating the output voltage v_o and the flying capacitor voltages $v_{c,1}$ and $v_{c,2}$, the duty cycles of the command signals must be controlled. The Pulse Width Modulation technique plays the role of the basic control method in power electronics systems. In the traditional PWM control, the duty cycles of the command signals u_1, u_2, and u_3 are varied according to the error signals to control the output variables. The simplest analog form of generating fixed frequency PWM is by comparison with a linear slope waveform such as a triangular periodic signal in such a way that the output signal goes high/low when the control signal is higher/lower than the triangular signal. This is implemented using a comparator whose output voltage goes to a logic 1 when one input is greater than the other. Other signals with straight edges can be used for modulation. A failing ramp carrier will generate PWM with leading edge modulation. When the control signal s_k is smaller (resp. greater) than the sawtooth ramp voltage h_k, the switch is OFF (resp. ON). As the system contains three controlled switches, this modulation strategy should be applied for the three switches. The ramp carriers are phase shifted in such a way that the control signal s_1 is compared with the ramp carrier signal $h_1(t)$, the control signal s_2 is compared with $h_2(t) = h_1(t - T/3)$ while the signal s_3 is compared with the sawtooth ramp signal $h_3(t) = h_1(t - 2T/3)$, where T is the period of the ramp signal which coincides with the switching period. In the case of a digital PWM control, this will also be the sampling period.

Obtaining the expression of the control signals is challenging as the system is multi-input multi-output (MIMO). A MIMO control design may be the work of another research in this area and it is beyond the scope of this paper. We will consider here a purely proportional control with the aim to minimize the error

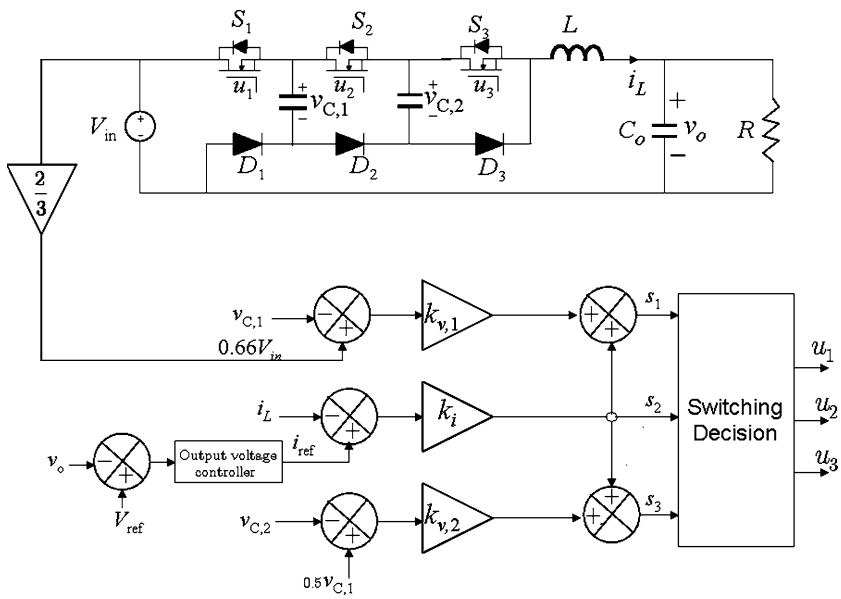

Fig. 2 Four-level DC–DC buck converter and its PWM MIMO controller

between the outputs and their references values. In order to control the voltage $v_{C,1}$ to $2v_{in}/3$, i_L to i_{ref} and $v_{C,2}$ to $v_{in}/3$, we consider the error signals $e_1 = 2V_{in}/3 - v_{c,1}$, $e_2 = i_{ref} - i_L$, and $e_3 = v_{c,2} - 0.5v_{c,1}$. Then, the control signals to be compared with the repetitive signals h_k are as follows:

$$\begin{aligned} s_1(\mathbf{x}) &= k_{v,1}e_1 + k_i e_2 \\ s_2(\mathbf{x}) &= k_i e_2 \\ s_1(\mathbf{x}) &= k_{v,2}e_3 + k_i e_2 \end{aligned} \tag{30}$$

where k_i, $k_{v,1}$, and $k_{v,2}$ are feedback coefficients. It is worth noting that due to the phase shift among the repetitive signals h_k, two of the switching instants are synchronous and are given in a fixed pattern. These are $t_2 = T/3$ and $t_4 = 2T/3$. The other remaining switching instants are asynchronous and they are obtained as the solution of the equation resulting from the crossing of the control signals s_k with the ramp periodic functions h_k. These periodic functions have the following expressions:

$$\begin{aligned} h_1(t) &= V_u - (V_u - V_l)\frac{t}{T} \mod 1 \\ h_2(t) &= V_u - (V_u - V_l)\frac{t - T/3}{T} \mod 1 \\ h_3(t) &= V_u - (V_u - V_l)\frac{t - 2T/3}{T} \mod 1 \end{aligned} \tag{31}$$

In order to get an output voltage regulation, the signal i_{ref} is taken from the output voltage controller. If a purely proportional controller is used, this reference current is given by:

$$i_{ref} = k_o(V_{ref} - v_o) \tag{32}$$

where k_o is the proportional gain.

5.2 Orbital stability analysis

In order to perform the orbital stability analysis of the earlier-described system, let us choose the following values of the parameters: input voltage $V_{in} = 30\,\mathrm{V}$, capacitance $C_1 = 20\,\mu\mathrm{F}$, capacitance $C_2 = 20\,\mu\mathrm{F}$, output capacitance $C_o = 20\,\mu\mathrm{F}$, inductance $L = 100\,\mu\mathrm{H}$, load resistance $R = 5\,\Omega$, reference voltage $V_{ref} = 20\,\mathrm{V}$,[1] switching period is selected to be $T = 50\,\mu\mathrm{s}$. The lower and the upper values of the repetitive voltages are $V_l = 0$ and $V_u = 5\,\mathrm{V}$. The feedback coefficients k_i and k_o are set to 1, $k_{v,}1$ and $k_{v,}2$ are taken equal: $k_{v,1} = k_{v,2} = k_v$ and k_v is considered as a design parameter that should be adjusted to obtain a stable behavior. The switching sequence is the following: $C_1 \rightarrow C_2 \rightarrow C_3 \rightarrow C_4 \rightarrow C_5 \rightarrow C_6$, which corresponds to $(u_1, u_2, u_3) = \{(0, 1, 0), (0, 1, 1) (0, 0, 1), (1, 0, 1), (1, 0, 0)$ and $(1, 1, 0)\}$. This sequence gives rise to a 6-modal periodic orbit in the stationary state. Figure 3 shows the time-domain waveforms of the 6-modal periodic orbit. The results are obtained both from direct time-domain simulation and by means of reconstructing the data from the fixed point of the Poincaré map. As can be seen, there is a good concordance between the results. In order to study the stability of this orbit, the loci of the eigenvalues $\lambda(\mathbf{DP})$ of the Jacobian matrix **DP** are plotted when the parameter k_v is increased. This parameter is swept in the range (0.2, 1.6). The results are shown in Fig. 4a. From the locus of the eigenvalues, we can deduce that the system presents a FB as the parameter k_v is increased. Since one of the eigenvalues crosses the unit circle from $(-1, 0)$ at a critical value of $k_{v,}\mathrm{cri} \approx 0.85$, it is expected that the system undergoes a FB at this point. Time-domain simulations using exact circuit description are used to check the results. Figure 4b shows the bifurcation diagram of the inductor current. It can be observed that the critical value of the k_v is $k_{v,}\mathrm{cri} \approx 0.85$. This value agrees well with the result obtained from the stability analysis based on the Jacobian matrix of the Poincaré map. However, note that after the 6-modal periodic orbit loses its stability by a smooth FB, some nonsmooth bifurcations in the form of a border collision (BC) can occur afterwards. These BC bifurcations take place due to the fact that the system loses smoothness for a certain value of the bifurcation parameter.

The loss of smoothness is due to a structural change in the model of the system. More specifically, the saturation of the command input u_k during some cycles is the main cause of nonsmoothness. NSB can also take place for other bifurcation parameters or for other values of the fixed parameters. For instance, if the output capacitance C_o is relatively small, the system has the tendency to lose stability by a NSB. Figure 5a shows the loci of the eigenvalues as the bifurcation param-

[1] Note that the use of a purely proportional controller will introduce a static error in the output voltage whose average value will be less than V_{ref}. In our case, the duty cycles obtained taking into account the static error are in the range of (33, 50)%.

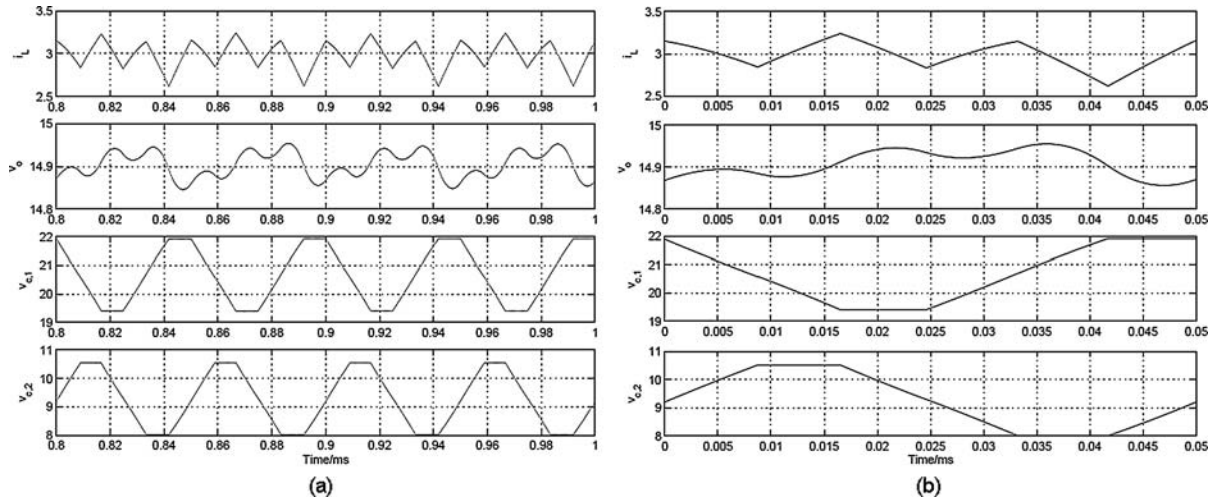

Fig. 3 Stationary periodic waveforms of the state variables (**a**) from simulation of the switched model during four switching periods (transient was removed) and (**b**) from the reconstruction of the fixed point of the Poincaré map during one switching cycle

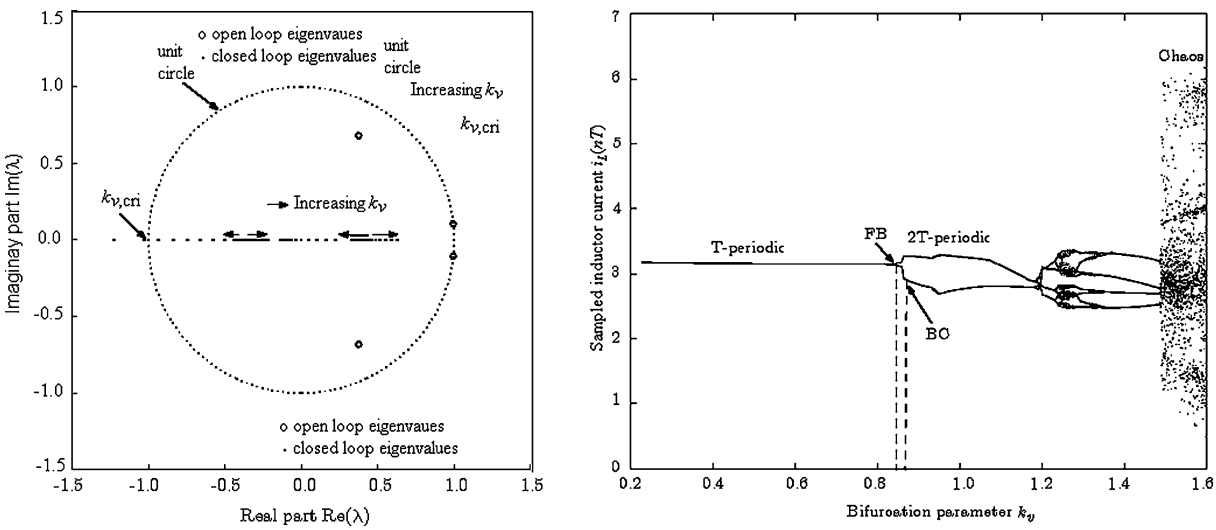

Fig. 4 (**a**) Eigenvalues loci of the Jacobian matrix of the Poincaré map corresponding to a four-level converter as the parameter k_v is increased. The eigenvalues of the open loop system are also indicated by *small circles*. (**b**) Bifurcation diagram taking k_v as a bifurcation parameter showing a FB

eters as the bifurcation parameter k_v is swept in the same range as before but with $C_o = 10\,\mu$F. However, in this case, two of the eigenvalues of the closed-loop system crossing the unit circle are complex conjugates. The bifurcation diagram of this case is shown in Fig. 5b, where a NSB can be observed. After this bifurcation, the trajectory of the system in the steady state is a torus and which with further changes in the bifurcation parameter can undergo a BC bifurcation resulting in a nonsmooth torus (quasiperiodic behavior or phase-locked loop) or in a chaotic attractor. Note that in order to explain the nonsmooth torus breakdown, the model should take into account the saturation effect of the duty cycles. Clearly, our model used to derive the Jacobian matrix does not include such effect and cannot explain the border collision bifurcations. However in the saturation region, the corresponding Poincaré map model is linear because the switching instants are constants and do not depend on the state variables. The linearization of the Poincaré map in the

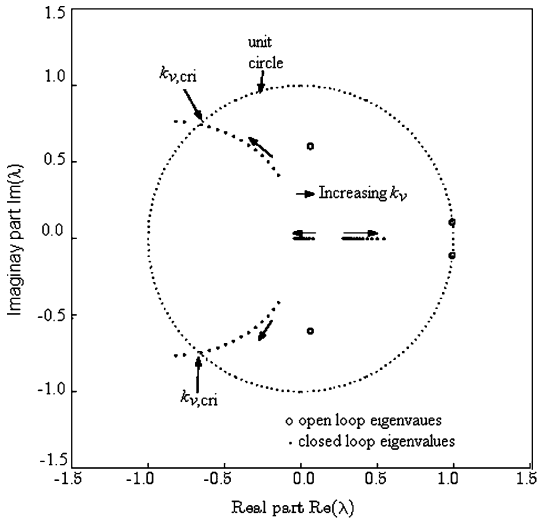

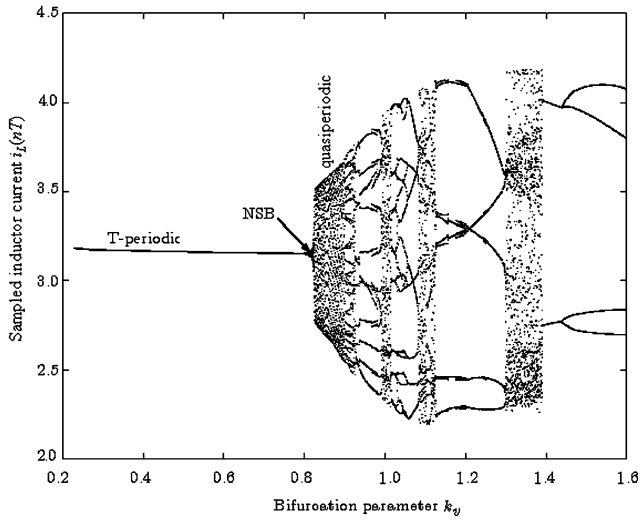

Fig. 5 (**a**) Eigenvalues loci of the Jacobian matrix of the Poincaré map corresponding to a four-level converter as the parameter k_v is increased. The eigenvalues of the open-loop system are also indicated by *small circles*. $C_o = 10\,\mu$F. (b) Bifurcation diagram taking k_v as a bifurcation parameter showing a NSB

saturating and the nonsaturating regions will give rise to a piecewise affine map that could be used to analyze the nonsmooth bifurcation of high periodic orbits of the system. In this paper, we are considering only the first bifurcation since it is the most important from the design point of view. The analysis of the postbifurcations, most of them being classified in the category of BC bifurcations, is beyond the scope of this paper. Readers interested in the phenomenon of the border collision torus breakdown are referred to the recent papers [26, 27].

6 Conclusions

We have presented a systematic procedure to obtain the Poincaré map of MIMO DPWA dynamical systems with continuous state variables and discontinuous vector field. This model is in the form of a Poincaré map and it can be obtained by a composition of different local mappings built in local cells between two adjacent switching boundaries. We obtained that although the actual system is discontinuous, the corresponding Poincaré map is smooth if the number of configurations does not alter. In this case, only conventional bifurcations FB, NSB, and SN can take place. Bifurcations of the fixed points are closely related to the loss of stability when a parameter is varied. The Poincaré map can be used to study accurately the stability of periodic orbits of the switched system as obtained from its exact general continuous-time dynamical model. The expression of the fixed point and the Jacobian matrix are given in closed form in term of system matrices and steady state switching time instants. In closed-loop systems, these time instants can be obtained numerically by using a root finding algorithm. For instance, the least square method can be used. The methodology proposed in this work is a suitable systematic procedure to the analysis of the orbital stability of a DPWA system independently of its dimension and the number of its configurations. The combination of closed-form expressions and numerical procedures allows the analysis of the influence of the parameters on the behavior of the system. Details on computing some matrices and vectors appearing in the model are discussed. The proposed approach is applied to a nontrivial power electronic DC–DC converter which uses six configurations during one switching cycle. The results of the stability analysis by using the eigenvalues of the Jacobian matrix have been confirmed by time-domain simulations of the exact circuit diagram description. A good agreement between numerical simulation and theoretical prediction has been obtained. Most of nonlinear phenomena that are undergone by the nominal periodic orbit of DPWA switched systems are classified into standard bifurcations like FB, NSB, and SNB. In this paper, we have attempted to provide some analytical expressions to detect accurately these local bifurcations.

Other nonstandard bifurcations as, for example, BC bifurcations are also possible and they can only occur when the number of configurations during one switching cycle may vary or the switching sequence is modified. In our opinion, the formality and generality of our presentation are necessary because of their applicability to a wide class of switched systems. Future research aims to apply the approach to analyze the stability of general multilevel converters and to orient it to the system design using discrete time control theory. Global stability and experimental validation is also a subject of further study.

Appendix

1.1 Configurations of the four-level DC–DC buck converter

- Configuration C_1, (OFF, ON, OFF): During this configuration, the inductor L is discharged, capacitor C_2 is charged, and C_1 capacitor is discharged. The system matrix **A** and vector **B** for this configuration are:

$$\mathbf{A}_1 = \begin{pmatrix} 0 & -\frac{1}{L} & \frac{1}{L} & -\frac{1}{L} \\ \frac{1}{C_o} & -\frac{1}{RC_o} & 0 & 0 \\ -\frac{1}{C_1} & 0 & 0 & 0 \\ 0 & 0 & 0 & 0 \end{pmatrix}, \quad \mathrm{B}_1 = \begin{pmatrix} 0 \\ 0 \\ 0 \\ 0 \end{pmatrix} \tag{A.1}$$

- Configuration C_2, (OFF, ON, ON) During this configuration, the inductor L is charged, capacitor C_1 is still discharging, and C_2 capacitor charge is maintained. The system matrix **A** and vector **B** for this configuration are:

$$\mathbf{A}_2 = \begin{pmatrix} 0 & -\frac{1}{L} & \frac{1}{L} & 0 \\ \frac{1}{C_o} & -\frac{1}{RC_o} & 0 & 0 \\ -\frac{1}{C_1} & 0 & 0 & 0 \\ 0 & 0 & 0 & 0 \end{pmatrix}, \quad \mathrm{B}_2 = \begin{pmatrix} 0 \\ 0 \\ 0 \\ 0 \end{pmatrix} \tag{A.2}$$

- Configuration C_3, (OFF, OFF, OFF): During this configuration, the inductor L is discharged, capacitor C_1 and C_2 charges are maintained. The system matrix **A** and vector **B** for this configuration are:

$$\mathbf{A}_3 = \begin{pmatrix} 0 & -\frac{1}{L} & 0 & \frac{1}{L} \\ \frac{1}{C_o} & -\frac{1}{RC_o} & 0 & 0 \\ 0 & 0 & 0 & 0 \\ 0 & 0 & 0 & 0 \end{pmatrix}, \quad \mathrm{B}_3 = \begin{pmatrix} 0 \\ 0 \\ 0 \\ 0 \end{pmatrix} \tag{A.3}$$

- Configuration C_4, (ON, OFF, ON): During this configuration, the inductor L and capacitor L_1 are charged while capacitor L_2 is discharged. The system matrix **A** and vector **B** for this configuration are:

$$\mathbf{A}_4 = \begin{pmatrix} 0 & -\frac{1}{L} & \frac{1}{L} & \frac{1}{L} \\ \frac{1}{C_o} & -\frac{1}{RC_o} & 0 & 0 \\ 0 & 0 & 0 & 0 \\ -\frac{1}{C_2} & 0 & 0 & 0 \end{pmatrix}, \quad \mathrm{B}_4 = \begin{pmatrix} \frac{V_{\mathrm{in}}}{L} \\ 0 \\ 0 \\ 0 \end{pmatrix} \tag{A.4}$$

- Configuration C_5,(ON, OFF, OFF): During this configuration, the inductor L is discharged, capacitor L_1 is still charging, and L_2 capacitor charge is maintained. The system matrix **A** and vector **B** for this configuration are:

$$\mathbf{A}_5 = \begin{pmatrix} 0 & -\frac{1}{L} & -\frac{1}{L} & 0 \\ \frac{1}{C_o} & -\frac{1}{RC_o} & 0 & 0 \\ \frac{1}{C_1} & 0 & 0 & 0 \\ 0 & 0 & 0 & 0 \end{pmatrix}, \quad \mathrm{B}_5 = \begin{pmatrix} \frac{V_{\mathrm{in}}}{L} \\ 0 \\ 0 \\ 0 \end{pmatrix} \tag{A.5}$$

- Configuration C_6, (ON, ON, OFF): During this configuration, the inductor is charged the L_1 capacitor charge is maintained while L_2 is charged. The system matrix **A** and vector **B** for this configuration are:

$$\mathbf{A}_6 = \begin{pmatrix} 0 & -\frac{1}{L} & 0 & -\frac{1}{L} \\ \frac{1}{C_o} & -\frac{1}{RC_o} & 0 & 0 \\ 0 & 0 & 0 & 0 \\ \frac{1}{C_2} & 0 & 0 & 0 \end{pmatrix}, \quad \mathrm{B}_6 = \begin{pmatrix} \frac{V_{\mathrm{in}}}{L} \\ 0 \\ 0 \\ 0 \end{pmatrix} \tag{A.6}$$

1.2 Switching functions σ_k for the four-level DC–DC buck converter

The switching instants t_k are given by solving the equation resulting from the crossing of the repetitive periodic signals hk with the control signals s_k. These control signals are given by:

$$\begin{aligned} s_1(\mathbf{x}) &= k_{v,1}e_1 + k_i e_2 \\ s_2(\mathbf{x}) &= k_i e_2 \\ s_1(\mathbf{x}) &= k_{v,2}e_3 + k_i e_2 \\ &. \end{aligned} \tag{A.7}$$

In compact form, the control signals s_k can be written as:

$$s_k(\mathbf{x}) = \mathbf{K}_k(\mathbf{X}_{\mathrm{ref},k} - \mathbf{x}) \tag{A.8}$$

where $\mathbf{K}_k$ are the vector of feedback coefficients that will be given later and $\mathbf{X}_{\mathrm{ref},k}$ are the vector of the reference values of the output variables during the kth subinterval that are given by:

$$\mathbf{X}_{\mathrm{ref},1} = \begin{pmatrix} 0 \\ V_{\mathrm{ref}} \\ 0.66V_{\mathrm{in}} \\ 0 \end{pmatrix}, \quad \mathbf{X}_{\mathrm{ref},2} = \begin{pmatrix} 0 \\ V_{\mathrm{ref}} \\ 0 \\ 0 \end{pmatrix},$$

$$\mathbf{X}_{\mathrm{ref},3} = \mathbf{X}_{\mathrm{ref},2} \tag{A.9}$$

Note that some elements in the $\mathbf{X}_{\mathrm{ref}}$ and $\mathbf{K}_k$ vector are null because only some of the state variables are to be controlled by feedback. The remaining state variables will be directly related to these controlled variables.

The control signals are compared with three sawtooth signals with lower value V_l, upper value V_u, period T and providing $2\pi/3$ phase shift among them. The expressions of the switching functions are as follows:

$$\begin{aligned} \sigma_1(t, \mathbf{x}) &= s_1(\mathbf{x}) - h_1(t) \\ \sigma_2(t, \mathbf{x}) &= s_2(\mathbf{x}) - h_2(t) \\ \sigma_3(t, \mathbf{x}) &= s_3(\mathbf{x}) - h_3(t). \end{aligned} \tag{A.10}$$

The expressions for the vector of the feedback vectors $\mathbf{K}_k$ are given by:

$$\begin{aligned} \mathbf{K}_1 &= (\,k_i \;\; -k_i k_o \;\; k_{v,1} \;\; 0\,) \\ \mathbf{K}_2 &= (\,k_i \;\; -k_i k_o \;\; 0 \;\; 0\,) \\ \mathbf{K}_3 &= (\,k_i \;\; -k_i k_o \;\; 0.5k_{v,2} \;\; k_{v,2}\,) \end{aligned} \tag{A.11}$$

Acknowledgments The author would like to thank the anonymous reviewer who carefully reviewed the paper and provided helpful comments to improve it.

References

1. Armanazy, A.N.: Steady-state analysis of piecewise-linear systems with periodic inputs. Proc. IEEE **61**, 789–790 (1973)
2. Pettit, N.B.O.L., Wellstead, P.E.: Analyzing piecewise linear dynamical systems. IEEE Control Syst. Mag. **15**(5), 43–50 (1995)
3. Johansson, M., Rantzer, A.: Computation of piecewise quadratic Lyapunov functions for hybrid systems. IEEE Trans. Autom. Control **43**(4), 555–559 (1998)
4. Imura, J.I., van der Schaft, A.: Characterization of well-posedness of piecewise-linear systems. IEEE Trans. Autom. Control **45**(9), 1600–1619 (2000)
5. Doi, S., Kumagai, S.: Complicated slow oscillations with simple switching dynamics in a piecewise linear neuronal model. In: Proceedings of The 47th IEEE International Midwest Symposium on Circuits and Systems II, Hiroshima, Japan, pp. 609–612 (2004)
6. Chua, L., Deng, A.: Canonical piecewise-linear modeling. IEEE Trans. Circuits Syst. **33**(5), 511–525 (1986)
7. Liberzon, D.: Switching in Systems and Control. Oxford University Press, Oxford (1999)
8. Freire, E., Ponce, E., Rodrigo, F.: Torres, F., Bifurcation sets of continuous piecewise linear systems with two zones. Int. J. Bif. Chaos **8**(11), 2073–2097 (1998)
9. Leine, R.I., Nijmeijer, H.: Dynamics and Bifurcations of Non-Smooth Mechanical Systems. Springer-Verlag, Berlin (2004)
10. di Bernardo, M., Vasca, F.: On discrete time maps for the analysis of bifurcations and chaos in DC/DC converters. IEEE Trans. Circuits Syst. I **47**(2), 130–143 (2000)
11. Ma, Y., Kawakami, H., Tse, C.K.: Analysis of bifurcation in switched dynamical systems with periodically moving border: Application to power converters. In: Proceedings of the IEEE International Symposium on Circuits and Systems (ISCAS'04), Vancouver, Canada, pp. 701–704 (2004)
12. Olivar, G., Fossas, E., Batlle, C.: Bifurcations and chaos in converters. Discontinuous vector fields and singular Poincaré maps. Nonlinearity **13**, 1095–1121 (2000)
13. Banerjee, S., Ranjan, P., Grebogi, C.: Bifurcations in two-dimensional piecewise smooth maps: theory and applications in switching circuits. IEEE Trans. Circuits Syst. I **47**(5), 633–643 (2000)
14. Mazumder, S.K., Nayfeh, A.H., Boroyevich, D.: Theoretical and experimental investigation of the fast-and slow-scale instabilities of a DC–DC converter. IEEE Trans. Power Electron. **16**(2), 201–216 (2001)
15. Fang, C.-C., Abed, E.H.: Robust feedback stabilization of limit cycles in PWM DC–DC converters. Nonlinear Dyn. **27**(3), 295–309 (2002)
16. El Aroudi, A., Debbat, M., Olivar, G., Benadero, L., Toribio, E., Giral, R.: Bifurcations in DC–DC switching converters:

review of methods and applications. Int. J. Bif. Chaos **15**(5), 1549–1578 (2005)
17. El Aroudi, A., Robert, B.: Modeling and dynamics of a high voltage DC–DC converter: a nonlinear approach. In: Proceedings of the International Symposium on Nonlinear Theory and its Applications, NOLTA04, Fukuoka, Japan, pp. 311–316 (2004)
18. El Aroudi, A., Debbat, M., Giral, R., Martínez-Salamero, L.: Stability analysis of piecewise linear differential equations. In: Congreso de Ecuaciones Diferenciales y Aplicaciones, CEDYA, Tarragona, Spain, CD-ROM (2003)
19. Roll, J.: Local and Piecewise Affine Approaches to System Identification. Ph.D. Thesis, Linköping Universitet, Linkopping, Sweden (2003)
20. Utkin, V.I., Guldner, J., Shi, J.: Sliding Mode Control in Electromechanical Systems. Taylor and Francis, London (1999)
21. Hang, J.Y., Gao, W., Hung, J.C.: Variable structure control: A survey. IEEE Trans. Ind. Electron. **40**(1), 2 (1993)
22. Efe, M.Ö., Ünsal, C., Kaynak, O., Yu, X.: Variable structure control of a class of uncertain systems. Automatica **40**, 59–64 (2004)
23. Meynard, T.A., Fadel, M., Aouda, N.: Modeling of mutlilevel converters. IEEE Trans. Ind. Electron. **44**(3), 356–364 (1997)
24. di Bernardo, M., Budd, C.J., Champneys, A.R.: Corner collision implies border-collision bifurcation. Physica D **154**, 171–194 (2001)
25. Hamill, D.C., Deane, J.H.B., Jefferies, D.J.: Modeling of chaotic DC–DC converters by iterated nonlinear mappings. IEEE Trans. Power Electron. **7**(1), 25–36 (1992)
26. Zhusubaliyev, Z.T., Moskilde, E.: Torus Birth Bifurcations in a DC/DC Converter. IEEE Trans. Circuits Syst. I **53**(8), 1839–1850 (2006)
27. Zhusubaliyev, Z.T., et al.: Border collision route to quasiperiodicity: Numerical investigation and experimental confirmation. Chaos **16**, 023122 (2006)